

## Simulation and Observation of the Long-Time Evolution of the Longitudinal Instability in a Cooler Storage Ring

O. Boine-Frankenheim, I. Hofmann, and G. Rumolo

*Gesellschaft für Schwerionenforschung (GSI), Planckstrasse 1, 64291 Darmstadt, Germany*

(Received 28 December 1998)

In the ESR heavy-ion cooler storage ring at GSI the exponential growth and the subsequent saturation phase of the longitudinal instability in space charge dominated ion beams can be monitored with high resolution. Kinetic simulations together with the experimental data lead to a new insight into the effects of space charge and electron cooling on the long-time evolution of the instability. In the simulations we observe the continuous excitation of long-lived collective modes generated by particle trapping in the self-excited potential, which suggest that previous “overshoot” concepts need revision. [S0031-9007(99)08941-3]

PACS numbers: 29.27.Bd, 29.20.Dh

Above a certain threshold beam intensity the interaction of a coasting charged particle beam with the electromagnetic fields induced in a ring environment can lead to self-amplification of an initial perturbation in beam current. This longitudinal instability leads to a rapid increase in the longitudinal momentum spread of the beam. It appears to be one of the main limiting factors in the longitudinal quality of intense coasting beams and the achievement of very short bunches in rings. For high energy beams in circular machines, where space charge effects are usually negligible, this phenomenon has been studied extensively by means of linear theory, kinetic simulation, and experiment [1,2]. Studies focused on the “overshoot phenomenon,” the dependence of the final phase space area on the initial momentum spread [3]. More recently attention was drawn to nonlinear wave phenomena in high energy beams [4,5]. In Ref. [5] a stationary BGK-like (Bernstein-Green-Kruskal-like) [6] collective mode excited by a resistive impedance was constructed, exhibiting a “hole” in the beam distribution function.

In the framework of the heavy-ion fusion driver study [7] and possible high current storage and buncher rings for different applications, new interest arose on the influence of space charge on the instability. The evolution of the instability can be strongly influenced by the presence of space charge. This was first pointed out in Ref. [8] by means of kinetic simulations. It was shown that the destructive effect of the longitudinal instability in the short-wavelength regime (“microwave” instability) on a space charge dominated beam is suppressed. This stabilization was attributed to the space charged induced coupling between higher modes up to the cutoff frequency  $c/b$  ( $b$  pipe radius,  $c$  speed of light). Experimental efforts at GSI focused on the instability of coasting beams in the long-wavelength range (wavelengths much longer than the pipe diameter) caused by the resistive impedance of the rf cavities in the ESR heavy-ion storage ring. In the long-wavelength range a broader spectrum of possible collective excitations can be expected than in the short-

wavelength range. In a recent experiment at GSI with a space charge dominated ion beam it was discovered that the longitudinal instability leads to long-lived coherent structures on the beam [9]. In order to understand the long-time evolution experimentally observed a kinetic simulation code is employed. The kinetic description used to model the longitudinal dynamics of a coasting beam interacting with the ring environment is described as follows.

Let  $\theta_0 = \omega_0$  be the angular frequency,  $v_0$  the velocity of the synchronous particle, and  $\theta_0 + \Delta\theta$  and  $v_0 + v_z$  the angular frequency and velocity of a nonsynchronous particle in a ring of radius  $R$ . The coordinates in a system comoving with the synchronous particle are

$$z = R\Delta\theta, \quad v_z = \dot{z} = R\Delta\dot{\theta}. \quad (1)$$

The kinetic description is based on the Vlasov-Fokker-Planck equation for the distribution function  $f(z, v_z, t)$  written in the frame comoving with the beam,

$$\begin{aligned} \frac{\partial f}{\partial t} + v_z \frac{\partial f}{\partial z} - \frac{q\eta}{\gamma_0 m} E_z \frac{\partial f}{\partial v_z} \\ = \beta_f \frac{\partial}{\partial v_z} (v_z f) + D \frac{\partial^2 f}{\partial v_z^2}, \end{aligned} \quad (2)$$

with the frequency slip factor  $\eta = 1/\gamma_i^2 - 1/\gamma^2$ , the relativistic factor  $\gamma_0 = 1/(1 - \beta_0^2)^{1/2}$ ,  $\beta_0 = v_0/c$ , the total longitudinal electric field  $E_z(z, t)$ , the ion charge  $q$ , and the ion mass  $m$ . The Vlasov part on the left-hand side of Eq. (2) describes the collective dynamics. The Fokker-Planck term on the right-hand side of Eq. (2) accounts for electron cooling, described by the cooling rate  $\beta_f$  and intrabeam scattering (IBS), described by the diffusion constant  $D$ . The line charge density  $\rho_L$  and the momentum spread  $\sigma = \Delta p/p_0$  are given through

$$\rho_L(z, t) = q \int_{-\infty}^{\infty} f dv_z, \quad (3)$$

$$\sigma^2 = \frac{1}{(\eta v_0)^2} \int_0^{2\pi R} \int_{-\infty}^{\infty} v_z^2 f dv_z dz. \quad (4)$$

Perturbations on the beam current induce electric fields that act back on the beam. The coupling between the beam and the ring environment is described in terms of the ring impedance  $Z_n$  acting at harmonics  $\omega_n = n\omega_0$  of the revolution frequency  $\omega_0$ ,

$$E_{nz} = -\frac{1}{2\pi R} Z_n I_n. \quad (5)$$

Here,  $I_n$  and  $E_{nz}$  denote the space harmonics of the beam current and of the resulting electric field. We consider two contributions to the total impedance,

$$Z_n = Z_c + Z_{sc} \\ = \frac{R_s}{1 + iQ(\omega_0/\omega_r - \omega_r/\omega_0)} - \frac{ingZ_0}{2\beta_0\gamma_0^2}. \quad (6)$$

$Z_c$  is a narrow band impedance due to the rf cavity (shunt impedance  $R_s$ , quality factor  $Q$ ), with an eigenfrequency  $\omega_r$  tuned close to the revolution frequency.  $Z_{sc}$  is the space charge impedance [ $Z_0 = 377 \Omega$ ,  $g = 0.5 + 2 \ln(b/a)$  (beam radius  $a$ )], which acts on all harmonics up to the cutoff wavelength  $2\pi b$ .

The instability growth time and the long-time evolution of the self-bunching amplitudes were measured in the experiment with  $1.65 \times 10^8 \text{ C}^{6+}$  ions at 340 MeV/u ( $Z_{sc} = -i700 \Omega$ ). After cooling the beam to a momentum spread of  $\sigma_0 = 1.1 \times 10^{-5}$ , the eigenfrequency of the rf cavity ( $R_s = 1300 \Omega$ ) was tuned near to the revo-

lution frequency, resulting in an operating point ( $Z_c, Z_{sc}$ ) well outside the linear theory stability boundary for a Maxwellian velocity distribution [9]. The archived initial momentum spread was typically a factor of 1.8 below the threshold momentum spread for instability. The beam current signal from a longitudinal beam monitor was sampled and stored with high resolution over 1 s. Figure 1 shows the measured exponential growth and steepening and decay of the slow wave accompanied by smaller wavelength structures. The decay of the first wave is followed by the excitation of a second wave resulting in a persistent coherent signal on the beam.

For the simulation of the long-time evolution we numerically integrate Eq. (2) together with Eq. (5) and the impedance Eq. (6). The integration is performed on a grid in longitudinal phase space, with  $-\pi R < z < \pi R$  and  $-\nu_{\max} < \nu_z < \nu_{\max}$ . One simulation time step  $\Delta t$  is split into several substeps. First, the Vlasov part is integrated by means of the well-known splitting scheme presented in Ref. [10]. Second, we correct for the Fokker-Planck term by means of a simple time-implicit scheme. An instructive comparison between such a direct integration scheme and a particle-in-cell (PIC) code can be found in Ref. [11]. For the purpose of resolving long-time behavior together with space charge phenomena the direct integration has the advantage of being "noiseless."

In Ref. [9] it was already shown that the measured instability growth times and current profiles up to the

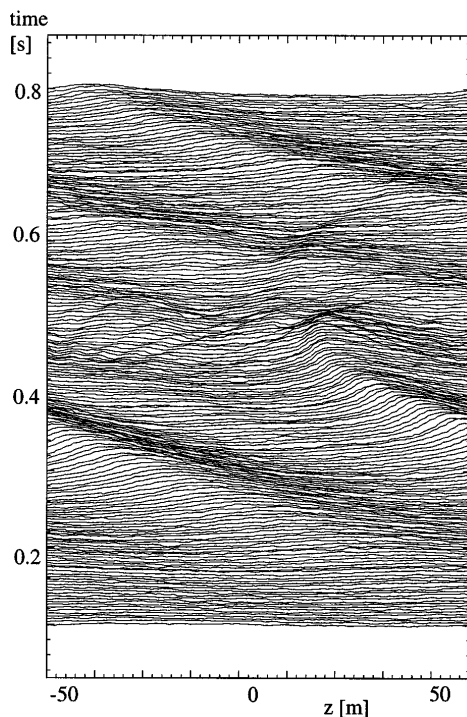


FIG. 1. Exponential growth and nonlinear saturation phase of the longitudinal resistive instability of a cooled coasting beam in the ESR driven by the rf cavity on the first harmonic. The plot shows subsequent time traces from bottom to top over 0.8 s (each trace is the line density profile over one revolution period).

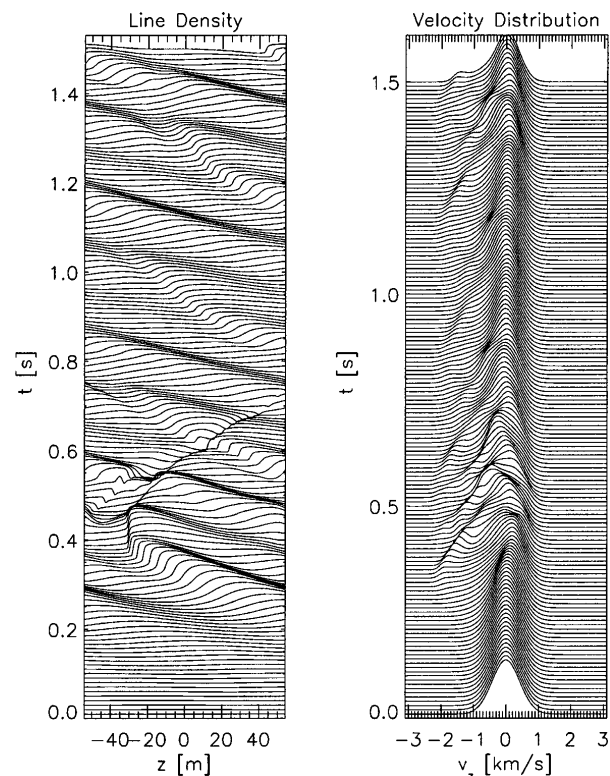


FIG. 2. Time evolution of the line density and velocity distribution obtained from the simulation.

first wave steepening are in good agreement with PIC simulations. For these simulations of the initial phase of the instability the effect of the electron cooling can be neglected due to the large cooling time relative to the instability growth times.

In the present work we employ the direct integration method and focus on the long-time behavior observed in the experiment. In the simulations we start from the initial conditions in the experiment, assuming a Maxwellian distribution function. We ignore the residual rf voltage present in the experiment. Therefore, the instability rise time will be slightly lower than in the experiment. The cooling time chosen is 400 ms, which is much longer than the instability rise time (40 ms). The measured initial equilibrium momentum spread together with the known cooling time gives us the approximate IBS diffusion coefficient  $D$ .

Figure 2 shows the time evolution of the line density and of the velocity distribution. In agreement with the experimental observation the simulation shows a persistent coherent signal on the beam. The velocity distribution does not converge to a stationary function either, but

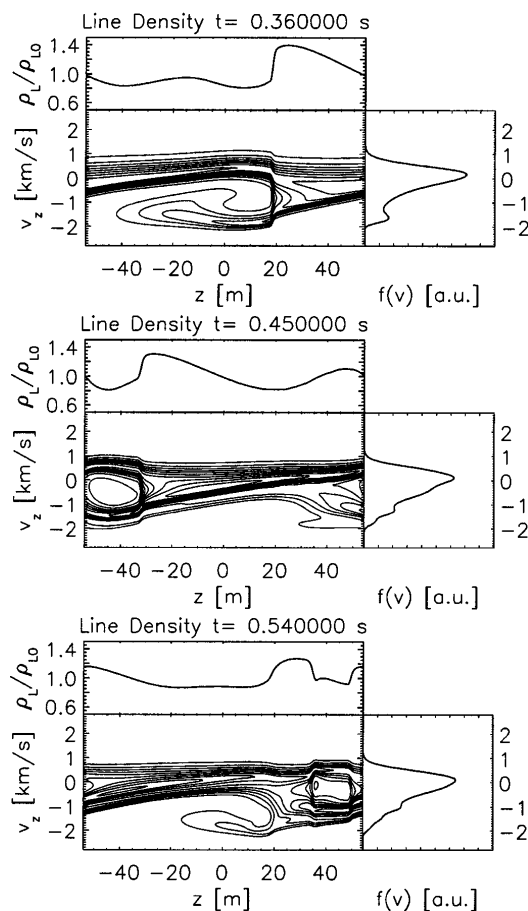


FIG. 3. Contour plot of the distribution function together with the corresponding line density and velocity distribution obtained from the simulation.

shows remaining fluctuations with a characteristic low-velocity “foot.”

In Fig. 3 snapshots of the distribution function together with the line charge density  $\rho_L$  (divided by the initial coasting beam value  $\rho_{L0}$ ) and the velocity distribution are shown. First the slow wave steepens and decays by trapping particles in the self-excited potential. The resulting hole structure has a lifetime of several hundred ms before it starts to smooth out due to IBS. During this period the hole causes localized line density dilutions. The excited hole structure can be regarded as a collective mode, similar to a traveling BGK wave [6] caused by nonlinear Landau damping [12] in ideal plasmas. In contrast to Ref. [5] we find that due to the presence of the resistive impedance a pure stationary BGK solution cannot be reached, even in the absence of IBS. The holes cause local current perturbations that continue to interact with the resistive impedance. Consequently, after the first saturation stage a second hole structure is excited (see Fig. 3). This hole formation continues in a cascade.

In Fig. 4 the resulting rms momentum spread evolution is shown (with cooling). The fluctuations of the momentum spread are caused by the continuous generation of holes in connection with the cooling force. Although the cooling rate is much lower than the instability growth rate, the saturated momentum spread fluctuates about a level which is well below the instability threshold momentum spread predicted by the linear theory for a Maxwell velocity distribution. The operating point after the saturation of the instability lies well outside the stability boundary. This “nonlinear stabilization” is due to the presence of the electron cooling. Momentum spread growth is caused by particle trapping, which is a nonlinear phenomenon at finite self-bunching amplitude. The threshold momentum spread is found by equating the rise time of the instability and the cooling time. However, care must be taken since

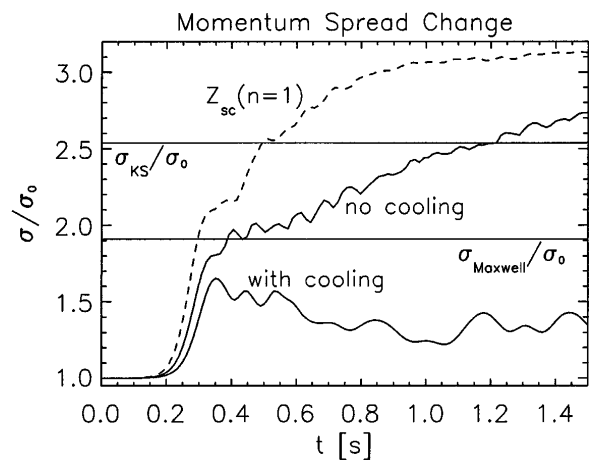


FIG. 4. Momentum spread change obtained from the simulation. The lower horizontal line is the threshold momentum spread for a Maxwellian velocity distribution and the upper line the threshold momentum spread following from the Keil-Schnell stability criterion.

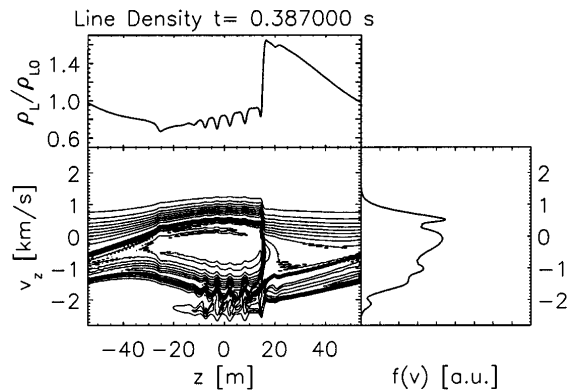


FIG. 5. Contour plot of the distribution function together with the corresponding line density and velocity distribution obtained from the simulation without cooling and diffusion.

the rise time at a finite self-bunching amplitude is much lower than during the initial linear stage. Therefore the momentum spread can saturate well below the threshold value predicted by linear theory.

To demonstrate the effect of cooling we switch off cooling and diffusion in the simulation. The resulting momentum spread (shown in Fig. 4) first seems to saturate about the threshold momentum spread, but then starts increasing continuously with a nearly linearly slope.

This continuous momentum spread growth is due to the subsequent generation of new long-lived hole structures. Figure 5 shows the generation of a second hole accompanied by short-wavelength structures, caused by space charge induced instabilities at higher harmonics. Without cooling and diffusion the wave steepening is more pronounced and higher order harmonics are stronger populated. It is noted that without cooling the momentum spread increase is accompanied by a decrease of the mean beam velocity.

In order to point out the effect of space charge on the time evolution of the instability we consider the same initial operating point, but with an imaginary impedance acting at harmonic  $n = 1$  only. Thereby the space charge induced coupling of different harmonics is switched off artificially. The resulting momentum spread (see Fig. 4), without cooling and IBS, rapidly saturates at a level above the threshold momentum spread following from the Keil-Schnell stability criterion [2]. This is the well-known “overshoot” behavior described in several former works [3]. Figure 6 shows that without space charge the self-bunching amplitudes during the exponential growth phase are much larger and no wave steepening occurs. In contrast to the evolution including space charge the effect of the instability is more destructive and no long-lived

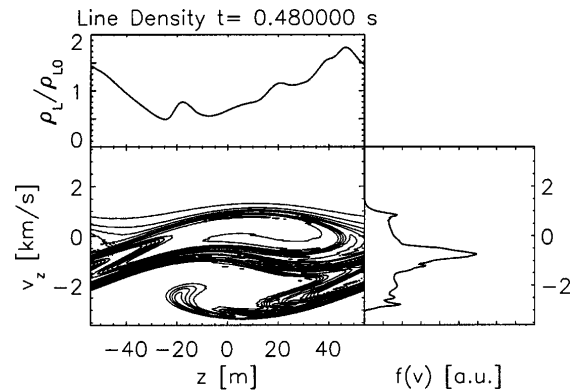


FIG. 6. Contour plot of the distribution function together with the corresponding line density and velocity distribution obtained from the simulation with space charge “switched off.”

hole structures are observed. The instability causes the rapid filamentation of the distribution function and within 900 ms a saturated, uniform line density results.

In summary we find a strongly modified time evolution of the instability for space charge dominated beams in storage rings. With space charge the evolution is dominated by long-lived hole structures and the overshoot behavior of the momentum spread is suppressed. Electron cooling can limit the momentum spread to values below the threshold value.

- 
- [1] V. K. Neil and A. M. Sessler, *Rev. Sci. Instrum.* **32**, 256 (1961); B. Zotter and P. Bramham, *IEEE Trans. Nucl. Sci.* **20**, 830 (1973); E. Keil and E. Messerschmid, *Nucl. Instrum. Methods* **128**, 203 (1975).
  - [2] E. Keil and W. Schnell, CERN Report No. ISR-TH-RF/69-48, CERN, 1969.
  - [3] R. A. Dori, MURA-Report **654** (1962); Y. Chin and K. Yokoya, *Phys. Rev. D* **28**, 2141 (1983); S. A. Bogacz and K. Y. Ng, *Phys. Rev. D* **36**, 1538 (1987).
  - [4] P. L. Colestock, L. K. Spentzouris, and F. Ostiguy, in *Proceedings of the 1995 Particle Accelerator Conference* (IEEE, Dallas, 1996), p. 2757.
  - [5] H. Schamel, *Phys. Rev. Lett.* **79**, 2811 (1997).
  - [6] I. B. Bernstein *et al.*, *Phys. Rev.* **108**, 546 (1957).
  - [7] GSI Report No. 98-06, 1998, edited by I. Hofmann and G. Plass.
  - [8] I. Hofmann, *Laser Part. Beams* **3**, 1 (1985).
  - [9] G. Rumolo *et al.*, *Nucl. Instrum. Methods Phys. Res., Sect. A* **415**, 363 (1998).
  - [10] S. G. Chen and G. Knorr, *J. Comput. Phys.* **22**, 330 (1976).
  - [11] O. Boine-Frankenheim and J. D’Avanzo, *Phys. Plasmas* **3**, 792 (1996).
  - [12] G. Manfredi, *Phys. Rev. Lett.* **79**, 2815 (1997).